Int. J. Electrochem. Sci., 8 **(2013)** 5213 - 5222

International Journal of
ELECTROCHEMICAL
SCIENCE
www.electrochemsci.org

Structural and Morphological Characteristics of Copper-Alumina Nano-Composite

N. M. Deraz

Chemistry Department, College of Science, King Saud University, P.O. Box 2455, Riyadh 11451,
Saudi Arabia.
E-mail: nmderaz@yahoo.com

Received: 24 February 2013 / *Accepted:* 14 March 2013 / *Published:* 1 April 2013

The crystallite size, lattice constant and unit cell volume of copper- alumina nano- composite were determined by X-ray diffraction (XRD) technique. Various phases of copper supported on alumina were prepared in this study by combustion route. The morphological properties of as prepared copper-alumina were studied by scanning electron micrographs (SEM) technique. The results revealed that the combustion method led to formation of different copper phases with various valences depending upon the amount of fuel. The change in amount of fuel affects formation and crysatllinity of products. The as synthesized materials have spongy and fragile characteristics.

Keywords: XRD; SEM, Cu, Cu_2O, CuO, nano- particles.

1. INTRODUCTION

A burst of research activity is witnessed in recent years in the area of synthesis and fabrication of different size and shape of metal nano-particles. Nanometer sized particles display many interesting optical, electronic, magnetic and chemical properties yielding applications in biological nano-sensors, optoelectronics, nano-devices, nano-electronics, information storage and catalysis [1]. Amongst many metals like Au, Ag, Pd, Pt, towards which research is directed, copper and copper compounds are the most important materials. The metallic Cu plays a significant role in modern electronics circuits due to its excellent electrical conductivity and low cost nano-particles [2]. So Cu will gain increasing importance as is expected to be an essential component in the future nano-devices due to its excellent conductivity as well as good biocompatibility and its surface enhanced Raman scattering (SERS) activity [3]. Metallic copper nano-crystals homogeneously dispersed in silica layers have attracted great attention recently for the development of nonlinear optical devices [4]. However, copper oxides attract the most attention because of their wide spread applications. Copper oxides are used in thin-film oxygen pressure sensors, as a binder in pastes for thick-film microelectronic circuits, as a p-type semiconductor, and they exhibit luminescence [5, 6]. But the most important application of copper oxide particles is as high surface area catalysts that are used in diverse experimental and industrial processes [7-10].

In the light of fast and growing applications of metallic copper and copper oxides nano-particles, a reproductive method of synthesis with a specific size, well defined surface composition, isolable and re-dispersible properties remains a challenging task to a synthetic chemist. The ability to scale up the synthesis to bulk scale will gain increasing importance as more applications are established. However, most of the synthetic methods either yielded particles of irregular shape with wide size distribution and required high temperature and pressure condition or produced particles with reduced catalytic activity and inability to reuse the particles [11].

In the current study, we aim to prepare copper- alumina nano- composite via glycine-assisted combustion method. Another goal for this investigation is the study of the effect of glycine content on the structural and morphological properties of the as prepared Cu/Al nano-composite. The techniques employed were XRD and SEM.

2. EXPERIMENTAL

2.1. Materials

Five samples of Cu/Al mixed oxides were prepared by mixing calculated proportions of copper and aluminum nitrates with different amounts of glycine. The mixed precursors were concentrated in a porcelain crucible on a hot plate at 400 ^{o}C for 5 minutes. The crystal water was gradually vaporized during heating and when a crucible temperature was reached, a great deal of foams produced and spark appeared at one corner which spread through the mass, yielding a brown voluminous and fluffy product in the container. In our experiment, the ratios of the glycine: aluminum: copper nitrates were (0, 2, 4, 6 and 8): 1: 2 for S1, S2, S3, S4 and S5 samples, respectively. In other words, the ratios of glycine to metal nitrates (G/N) were 0.00, 0.67, 1.33, 2.00 and 2.67 for S1, S2, S3, S4 and S5 samples. The chemicals employed in the present work were of analytical grade supplied by Fluke Company.

2.2. Techniques

An X-ray measurement of various mixed solids was carried out using a BRUKER D8 advance diffractometer (Germany). The patterns were run with Cu K_α radiation at 40 kV and 40 mA with scanning speed in 2θ of 2 ° min^{-1}.

The crystallite size of copper phases present in the investigated solids was based on X-ray diffraction line broadening and calculated by using Scherrer equation [12].

$$d = \frac{B\lambda}{\beta \cos\theta} \qquad (1)$$

where d is the average crystallite size of the phase under investigation, B is the Scherrer constant (0.89), λ is the wave length of X-ray beam used, β is the full-with half maximum (FWHM) of diffraction and θ is the Bragg's angle.

Scanning electron micrographs (SEM) were recorded on SEM-JEOL JAX-840A electron microanalyzer (Japan). The samples were dispersed in ethanol and then treated ultrasonically in order disperse individual particles over a gold grids.

3. RESULTS

3.1. Structural analysis

The preliminary investigation of the S1 sample showed that this sample consisted entirely of amorphous materials which may be copper and aluminum oxides and/or Cu-Al- O compound. The XRD pattern for S2, S3, S4 and S5 samples are given in Fig. 1. Study of this figure revealed that:

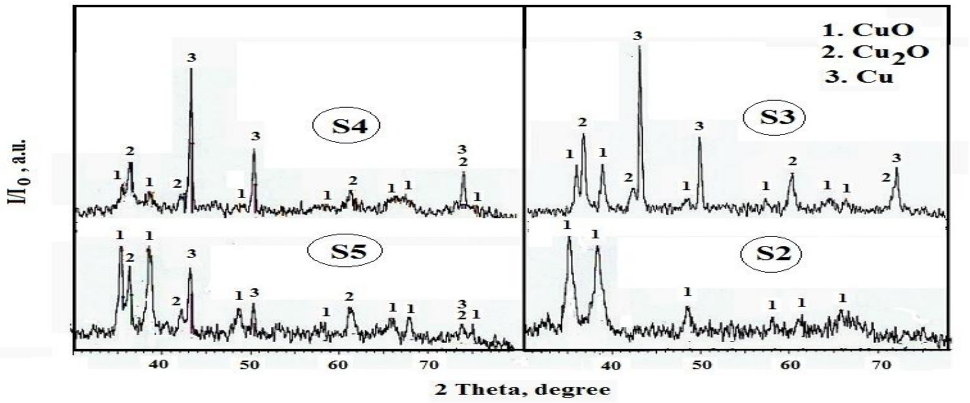

Figure 1. XRD patterns for the S1, S2, S3, S4 and S5 samples.

(i) The S2 sample consisted of moderate crystalline CuO particles as a single phase. This indicates that the presence of small amount of glycine (G/N = 0.67) led to crystallization of CuO particles (Tenorite, Monoclinic). (ii) The S3, S4 and S5 samples contain different phases of copper crystallites that are Cu, Cu_2O and CuO. This means that the presence of high amounts of glycine during the preparation process of Cu/Al composite resulted in reduction of some CuO to produce Cu (Cubic) and Cu_2O (Cuprite, Cubic) phases. When the G/N ratio was 1.33 or 2, the major phase was metallic copper. While the G/N ratio was 2.67, the major phase was CuO. (iii) The augmentation in the G/N ratio led to sharp the diffraction peaks of different crystalline phases. On the other hand, the increase in the G/N ratio from 1.33 to 2.67 brought about different changes in the intensities of different copper phases as shown in Table 1. This observation indicates the phase transformation and/or solid state reaction between copper and aluminum oxides producing amorphous $CuAl_2O_4$ and/or

$CuAlO_2$ particles. Indeed, the increase of G/N ratio from 1.33 to 2.67 resulted in a decrease in the peak height of metallic copper phase. Also, the increase of G/N ratio from 1.33 to 2.00 led to a decrease in the peaks height of both CuO and Cu_2O phases. Opposite behavior was observed for previous phases by increasing the G/N ratio up to 2.67. So, the increase in the G/N ratio affects the size and formation of products. In other words, judicious adjustment of the metal precursor- to-fuel ratio can control the size of reacting oxides and their solid reaction producing $CuAl_2O_4$ and $CuAlO_2$ nano-particles.

Table 1. The effect of glycine content on the height of some diffraction lines for the crystalline phase involved in the as prepared.

Samples	Crystalline Phases	Peak height (a. u.)		
		CuO (0.232nm)	Cu_2O (0.246nm)	Cu (0.209nm)
S1	-	-	-	-
S2	CuO	47	-	-
S3	CuO, Cu_2O, Cu	46	70	139
S4	CuO, Cu_2O, Cu	16	34	89
S5	CuO, Cu_2O, Cu	54	43	41

3.2. The size control of copper nano- crystals

The change in the ratio of glycine to metal nitrates brought about different changes in the crystallite size (d) of different copper phases as shown in Table 2. However, Table 2 shows the lattice constant (a) and unit cell volume (V) of Cu and Cu_2O nano- particles depending upon the X-ray data.

Table 2. Some structural parameters of cubic copper phases.

Samples	**Cu_2O**			**Cu**		
	d (nm)	a (nm)	V (nm^3)	d (nm)	a (nm)	V (nm^3)
S1	-	-	-	-	-	-
S2	-	-	-	-	-	-
S3	23	0.4277	7.824	43	0.3624	4.760
S4	14	0.4287	7.877	41	0.3626	4.768
S5	23	0.4279	7.835	35	0.3629	4.778

The increase in the glycine content brought about slightly changes in the values of crystallite size, lattice constant and unit cell volume of Cu_2O nano-crystals. On the other hand, this increase led to an increase in the values of lattice constant and unit cell volume for metallic copper crystallites. Opposite behavior was observed in the value of crystallite size of Cu nano- crystals.

3.3. The morphology study

The figures from 2A-B to 5A-B show the SEM images for S1, S2, S3 and S5 samples with different magnifications. The S1 sample contains agglomerated nano-particles. Addition of different amounts of glycine during the preparation process led to formation of spongy and fragile materials (the S2, S3 and S5 samples) containing voids and pores as shown in Figs 3-5. These voids and pores could be attributed to the release of large amounts of gases during combustion process depending upon the decomposition of glycine and copper and aluminum nitrates. In fact, the particle size of the S3 sample is higher than that of other samples. This confirms in Tables 1 and 2 depending upon the increase in the peaks height and crystallite size of the S3 sample. Also, we can be seen from the different SEM images that the agglomeration of the nano-particles of Cu/Al composite decreases as the G/N ratio increases. However, the increase in the G/N ratio brought about an increase in the homogeneity of particles for the composite studied.

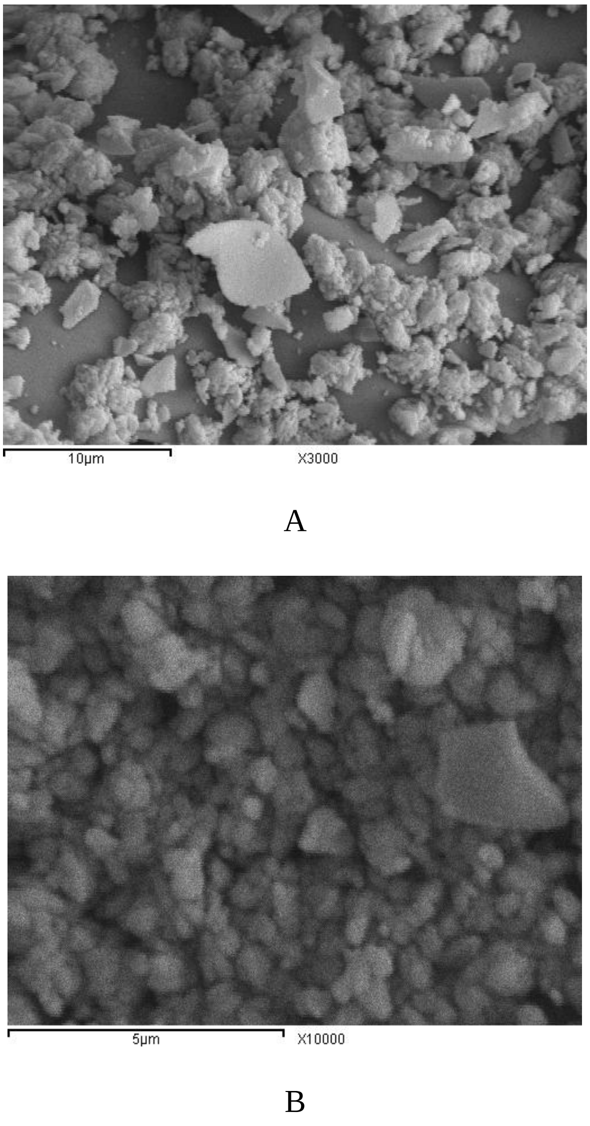

Figure 2. SEM image of the S1 sample with different magnifications.

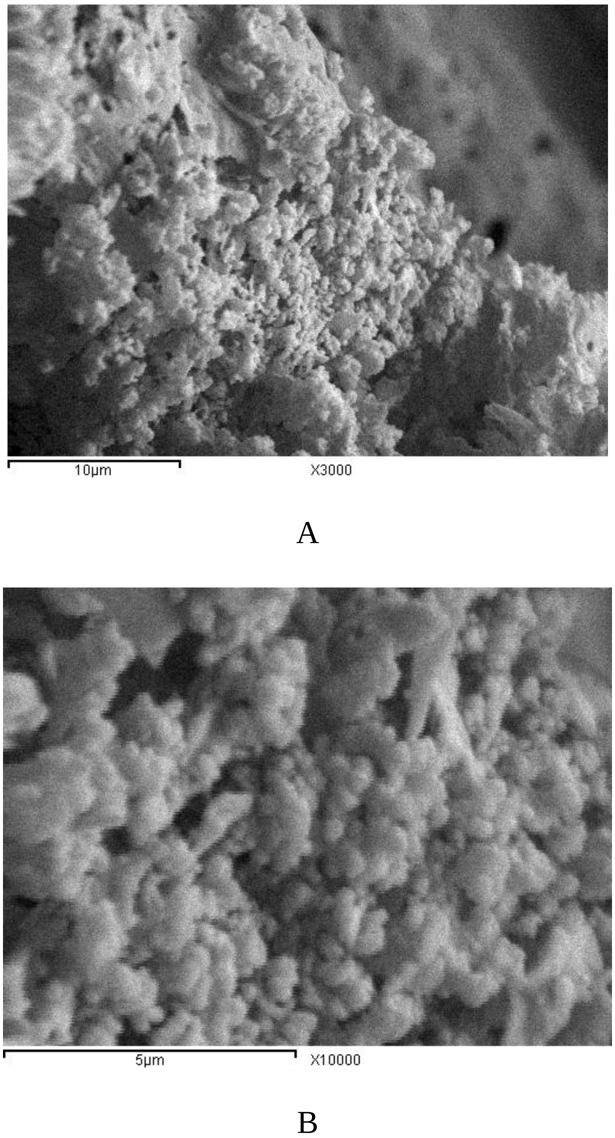

Figure 3. SEM image of the S2 sample with different magnifications.

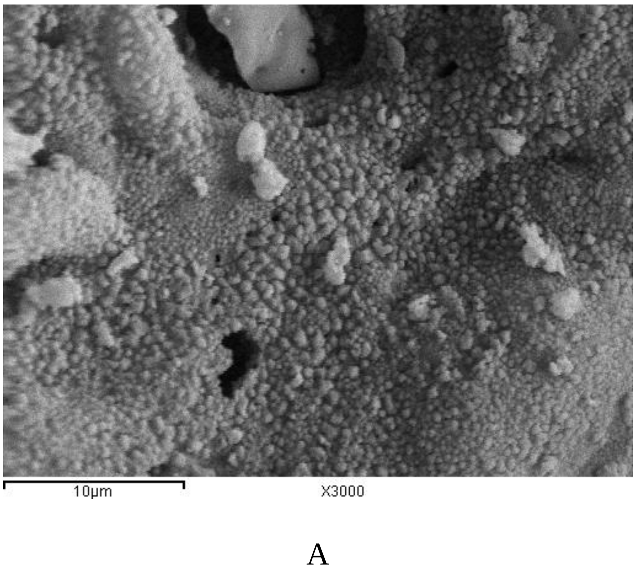

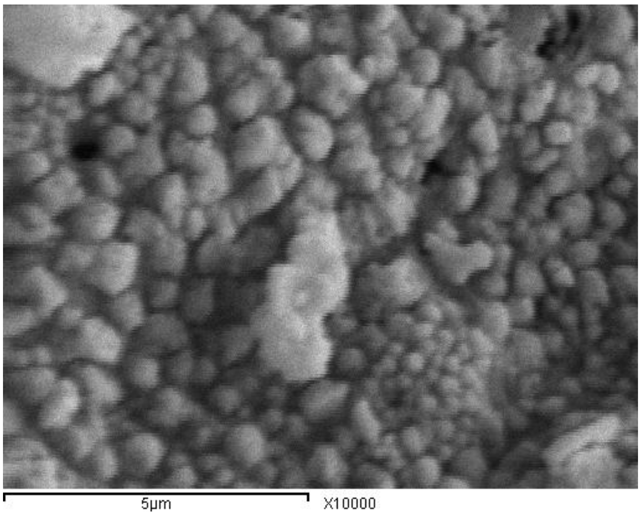

B

Figure 4. SEM image of the S3 sample with different magnifications.

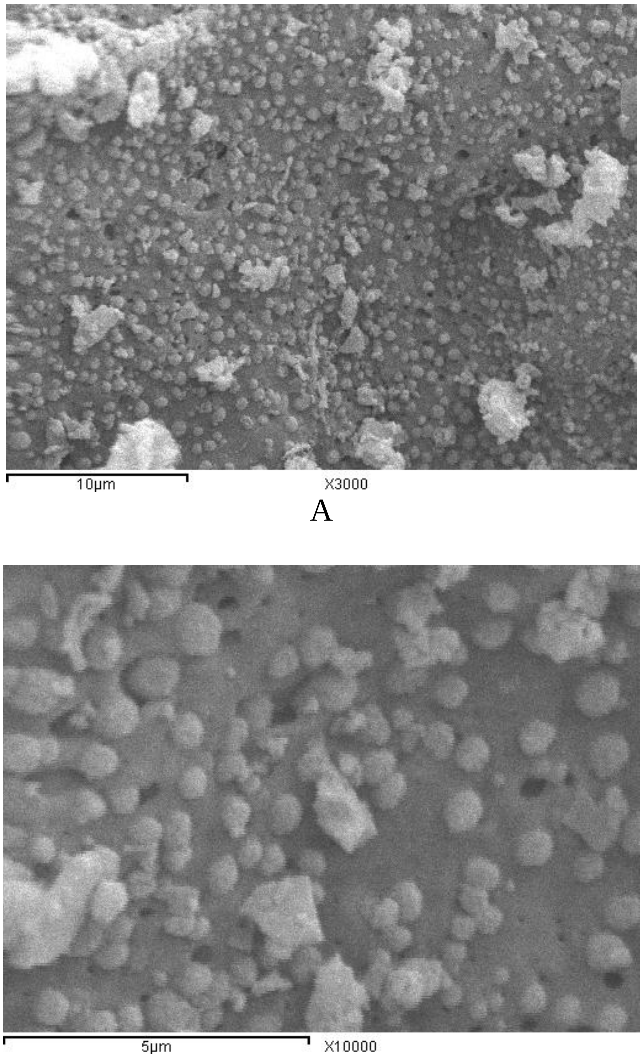

A

B

Figure 4. SEM image of the S5 sample with different magnifications.

4. DISCUSSION

Most metals exhibit high thermal conductivity depending upon the presence of free electrons. In addition, the electrical resistance of ceramics is usually high due to the lack of free electrons. However, heat transfer in ceramics occurs through the vibration of phonons. Combining thermally conductive metal and electrically insulating ceramic to form ceramic/metal aluminates may provide both high thermal conductance and high electrical resistance. But the ceramic/metal interface may act as a barrier to heat transfer [13]. The thermal resistance of the interface depends on its microstructure characteristics and the bonding technology employed. Many bonding techniques are available to bond alumina and copper. The solubility of oxygen in copper is very low. For example, it is only 0.03 at% at 1065 ^{o}C [14, 15]. As the amount of oxygen is higher than the solubility, Cu_2O is formed first then the CuO [16].

The chemical and structural relations of the Cu-Al-O system are more complex. Two oxides of copper can form in air: CuO (melaconite or tenorite) is the stable room-temperature oxide where the Cu ion is in the +2 valence state. Cu_2O (cuprite) where the Cu ion is in the +1 valence state is thermodynamically stable above 1020 °C. However, there are also two stable copper aluminates that can form in the C u-Al-O system: Cu(II)$A1_2O_4$ (spinel structure) and Cu(I)$A1O_2$ (delafossite structure) [17]. Phase equilibrium relations in the Cu_2O/CuO/ alumina system were determined experimentally by Gadalla and White [18]. Phase relations in this system have been calculated more recently by Jacob and Alcock [19]. In the present study, we found phase equilibrium relations in the Cu/Cu_2O/CuO/ alumina system. In other words, there are mixture of Cu, Cu_2O and CuO crystallites supported on the alumina surface. The presence of these crystallites is very important in the most catalytic reactions.

The XRD measurements for the S3, S4 and S5 samples show electron image recorded from a polycrystalline alumina substrate after reacting with CuO powder when the G/N ratio was 1.33-2.67, which is above the $Cu^{+2} \rightarrow Cu^{+1} + Cu^{0}$ transition temperature (1020 °C), and therefore Cu_2O and Cu were present in this sample [20]. The reaction equation was proposed as following:

$$4Cu^{+2} \rightarrow Cu^{+2} + Cu^{+1} + Cu^{0} \qquad (2)$$

Indeed, XRD measurements showed that the S2 sample consisted entirely of nano-crystalline CuO supported on amorphous alumina while the S3, S4 and S5 samples consisted of mixture of nano-crystalline CuO, Cu_2O and Cu supported on alumina surface. In addition, there are phase transformations between the copper phases depending upon the change in the crystallinity of these phases. Where, Cu phase was the major phase in the S3 and S4 samples while CuO was the major phase in the S5 phase due to the change in the G/N ratio.

One can not overcome the solid state reaction between copper and alumina yielding Cu-Al-O compounds [20]. This reaction depends upon the thermal diffusion for the cations of these oxides [21, 22]. Both $CuAl_2O_4$ and $CuAlO_2$ were found to form during reactions in air at 1100 °C between CuO powder and single-crystal alumina substrates. The relative position of the $CuAl_2O_4$and $CuAlO_2$ layers was observed to depend on the crystallographic orientation of the surface of the alumina substrate: $CuAl_2O_4$ formed in contact with (0001) alumina substrates while $CuAlO_2$ formed when the alumina substrate surface was (1120) [20]. Deraz reported that the glycine assisted combustion method is useful for providing an alternative of low cost mass production of various ceramic materials [21, 22]. The counter-diffusion of Cu^{2+}, Cu^{2+} and Al^{3+} through a relatively rigid aluminates film led to the formation of $CuAl_2O_4$ and/or $CuAlO_2$ nano-particles. In addition, following reactions indicate that Al_2O_3 decomposes to $2Al^{3+}$ and oxygen gas at Al_2O_3- interface. Moreover, oxygen moves through the reacted area to be added to the CuO interface and form spinel by reacting with aluminum ions:

At Al_2O_3 interface:

$$3Al_2O_3 + 2Cu^{2+} \rightarrow 2CuAl_2O_4 + 2Al^{3+} + 0.5O_2 \quad (3)$$

$$2Al_2O_3 + 2Cu^{1+} \rightarrow 2CuAlO_2 + 2Al^{3+} + O_2 \quad (4)$$

At CuO and Cu_2O interface:

$$2Al^{3+} + 3CuO + 0.5O_2 \rightarrow CuAl_2O_4 + 2Cu^{2+} \quad (5)$$

$$2Al^{3+} + 2Cu_2O + O_2 \rightarrow 2CuAlO_2 + 2Cu^{1+} \quad (6)$$

The morphology study of the investigated composites showed that these composites consist of polygonal- shaped grains with small incrustations on the surface. The presence of these incrustations is probably due to the influence of secondary phases. As the phase transformation of copper crystallites increases, the morphology has been modified and the grains are larger in size as shown in the S3 sample. The S5 sample shows a significant change in the morphological properties with the G/N ratio indicating to probability formation of Cu-Al-O compounds.

5. CONCLUSIONS

Effects of glycine content on the structural and morphological properties of Cu/Al nano-composite prepared by combustion method have been studied. The combustion route brought about the production of mixture of CuO, Cu_2O and Cu supported on alumina surface. The increase in the glycine content resulted in an increase in the lattice constant and unit cell volume of the produced CuO, Cu_2O and Cu involved in the investigated composite. But this treatment led to a decrease in the crystallite size for metallic copper and an increase in that for CuO and Cu_2O phases. The images of SEM showed that the as synthesized cobalt aluminates using high amounts of glycine has a significant porosity. The obtained samples have a homogenously distributed species in the whole mass prepared. The change in the G/N ratio resulted in change in the crystallinity of the mixture of CuO, Cu_2O and Cu involved in the composite studied.

ACKNOWLEDGEMENT

This project was supported by King Saud University, Deanship of Scientific Research, College of Science Research Centre.

References

1. D. L. Feldheim and C. A. Foss, Metal nano-particles: Synthesis, characterization and applications (Marcel Dekker Inc.) (eds) 2002 .
2. A. K. Schaper, H. Hou, A. Greiner, R. Schneider, F.Philips, *Appl. Phys. A Mater. Sci. Process* 78(2004)73.
3. B. Pergolese, M. Muniz-Miranda, A .Bigotto , *J. Phys.Chem. B,* 110 (2006)9241
4. C. J. Flytzanis , Physics B, *At. Mol. Opt. Phys.*, 38(2005)S661
5. H. Holzschuh and , H. Suhr, *J. Appl. Phys*. A, 51(1990)486.
6. D. Majumdar, T. A. Shefelbine, T. T Kodas, H. D. Glicksman, *J. Mat. Res*., 11(1996)2861.
7. K .Klier, *Adv. Catal*., 31(1982)243.
8. D. O.Klenov, , G. N Kryukova, L. M. Plyasova, *J. Mat. Chem.*, 8(1998)1665.
9. R. Pereia, M. Rufo, U. Schuchardt, *J. Braz. Chem. Society* 5(1994)83.
10. I. J. Shannon, F.Rey, G. Sankar, J. M. Thomas, T. Maschmeyer, A. M Waller, A. E. Palomares, A. Corma,., A. J. Dent and G. N. Greaves, *J. Chem. Soc. Faraday Trans*., 92(1996)4331.
11. H. Zhu, C. Zhang, Y. Yin, *Nanotechnology*, 16(2005) 3079.
12. B.D. Cullity, Elements of X-ray Diffraction, Addison-Wesly Publishing Co. Inc. 1976 (Chapter 14).
13. Shao-Kuan Lee, Wei-Hsing Tuan, Yin-Yin Wu, Shao-Ju Shih, *J. Euro. Ceram. Soc*., 33 (2013) 277.
14. K. P. Trumble, *Acta Metall. Mater.,* 40(1992)S105.
15. K. P. Trumble, *J. Am. Ceram. Soc., 82(1999)2912.*
16. A. Lupu, *J. Therm. Anal., 2(*1970)445.
17. T. Ishiguro, N. Ishizawa, N. Mizutani, M. Kato, *J. Solid State Chem.,* 41(1982)132.
18. A.M. Gadalla, J. White, *Trans. Brit. Ceram.* Soc., 63(1964)39.
19. K.T. Jacob, C.B. Alcock, *J. Am. Ceram. Soc.*, 58(1975)192.
20. David W. Susnitzky, C. Barry Carter, *J. Mater. Res*., 6(1991)1958
21. N. M. Deraz, *Ceramics International* 38 (2012) 511.
22. N. M. Deraz, *Int. J. Electrochem. Sci*. 7(2012) 4596.